Chemical Communications

COMMUNICATION

Tuning octahedral tilts and the polar nature of *A*-site deficient perovskites

Dashnor Beqiri, [a] Vanessa A. Cascos- Jiménez,[a] Jennie Roberts-Watts, [a] Ewan R. Clark,[a] Eric Bousquet,[b] Nicolas C. Bristowe[a] and Emma E. McCabe *[a]

Herein we highlight the ability to tune the structural chemistry of *A*-site deficient perovskite materials $Ln_{1/3}NbO_3$. Computational studies explore the balance between proper and hybrid-improper mechanisms for polar behaviour in these systems.

The three-dimensional (3D) connectivity of BO_6 octahedra in ABO_3 perovskites can result in a range of properties, including long-range magnetic or ferroelectric order, but there's been renewed interest in layered materials since the discovery of the hybrid improper mechanism for breaking inversion symmetry.[1-2] By this mechanism, combinations of non-polar distortions (e.g. octahedral tilts) can break inversion symmetry in layered materials, stabilising polar structures. These distortions can be considered as symmetry-breaking distortion modes applied to the parent high symmetry structure, whose amplitude indicates the magnitude of the distortion from the high symmetry model. These modes transform as an "irrep" (irreducible representation) depending on the symmetry change of the model as a result of the distortion.[3] This new "hybrid improper" mechanism contrasts with "proper" ferroelectrics for which the primary distortion mode is polar (i.e. the distortion from the high symmetry model to the ferroelectric state is driven by the softening of a polar distortion, rather than by combinations of non-polar distortions as for hybrid improper ferroelectrics). The *A*-site deficient perovskites $A_{1-x}BO_3$ (e.g. $Ln_{1/3}NbO_3$,[4] $Ln_{2/3}TiO_3$[5]) maintain the 3D connectivity of the *B* sublattice, but have layered ordering of *A* cations, giving some 2D character. This is illustrated by the high-temperature structure of $La_{1/3}NbO_3$ in which La^{3+} ions occupy two thirds of the *A* sites in alternate (001) layers.[4] This ordering is described by the X_3^- irrep[6] and in the absence of other distortions, gives the ideal structure of $P4/mmm$ symmetry (Figure 1(c)). Their layered nature makes $Ln_{1/3}BO_3$ perovskites ideal to study the balance between proper and hybrid-

improper mechanisms. Many adopt distorted structures with octahedral tilts tuned by Ln^{3+} ionic radius: $La_{1/3}TaO_3$ adopts the parent (untilted) $P4/mmm$ structure whilst with decreasing Ln^{3+} ionic radii, the structure distorts to allow first out-of-phase tilts about a single in-plane axis ($a^-b^0c^0$, $Cmmm$, $Ce_{1/3}TaO_3$ - $Gd_{1/3}TaO_3$), then about both in-plane axes ($a^-a^-c^0$, $Pbmm$, $Tb_{1/3}TaO_3$ and $Dy_{1/3}TaO_3$); for the smaller lanthanide analogues $Ho_{1/3}TaO_3$ and $Er_{1/3}TaO_3$, a polar crystal structure is adopted with tilts about in-plane and out-of-plane axes ($a^-a^-c^+$, $P2_1am$), allowing an in-plane polar displacement.[7] The range of niobates is limited, with only La, Pr and Nd reported to date.[4, 8]

The *A*-site vacancies in $Ln_{1/3}BO_3$ have made these systems a focus of research for Li^+ conductors *e.g.* $La_{(1-x)/3}Li_xNbO_3$[9] and $Ln_{2/3-x}Li_{3x}TiO_3$ (Ln = La, Nd).[10-11] However, reductive lithiation reactions, in which the *B* cations are partially reduced (e.g. $Li_xNd_{1/3}Nb^{5+}_{1-x}Nb^{4+}_xO_3$),[12] provide another route to tune structure and properties. In light of recent theoretical work, it's relevant to consider the polar nature of these materials and whether the balance between proper or improper can be tuned. This communication presents a combined experimental and theoretical approach to show that the $Ln_{1/3}BO_3$ series can be tuned from more proper-like to more improper with Ln radius, that lithiation is effective at tuning tilts and structural chemistry (by cation size factors), and that as such, these materials are worthy of further experimental and theoretical studies.

The parent niobate $Nd_{1/3}NbO_3$ was prepared† and room temperature high resolution neutron powder diffraction (NPD) data were indexed by an orthorhombic $2a_p \times 2a_p \times c_p$ unit cell (where a_p and c_p refer to the ideal $P4/mmm$ parent structure), consistent with the $Cmmm$ model ($a^-b^0c^0$ tilts) reported by Zhang et al.[8] Superstructure reflections that necessitate this larger unit cell (and result from octahedral tilts) are noticeably broader than the main reflections (see ESI) and a size-dependent broadening term was applied to them. This suggests a shorter correlation length (~50 Å) for this superstructure than for the cation sublattice. Refinement profiles and details are shown in Figure 1 (and ESI). These results confirm the out-of-centre displacement of the *B* site ions reported for $Nd_{1/3}NbO_3$[13] and $Ln_{1/3}TaO_3$[7] from X-ray powder diffraction data, with a significant displacement of Nb^{5+} ions towards the z = 0.5 layer with vacant *A* sites (Nb – O(2) = 1.8943(8) Å whilst Nb – O(1) = 2.0680(8) Å).

a. *School of Physical Sciences, University of Kent, Canterbury, Kent, CT2 7NH, U.K.*
b. *Université de Liège, Institut de Physique B5a, Allée du 6 Août, 17, B-4000 Sart Tilman, Belgium*
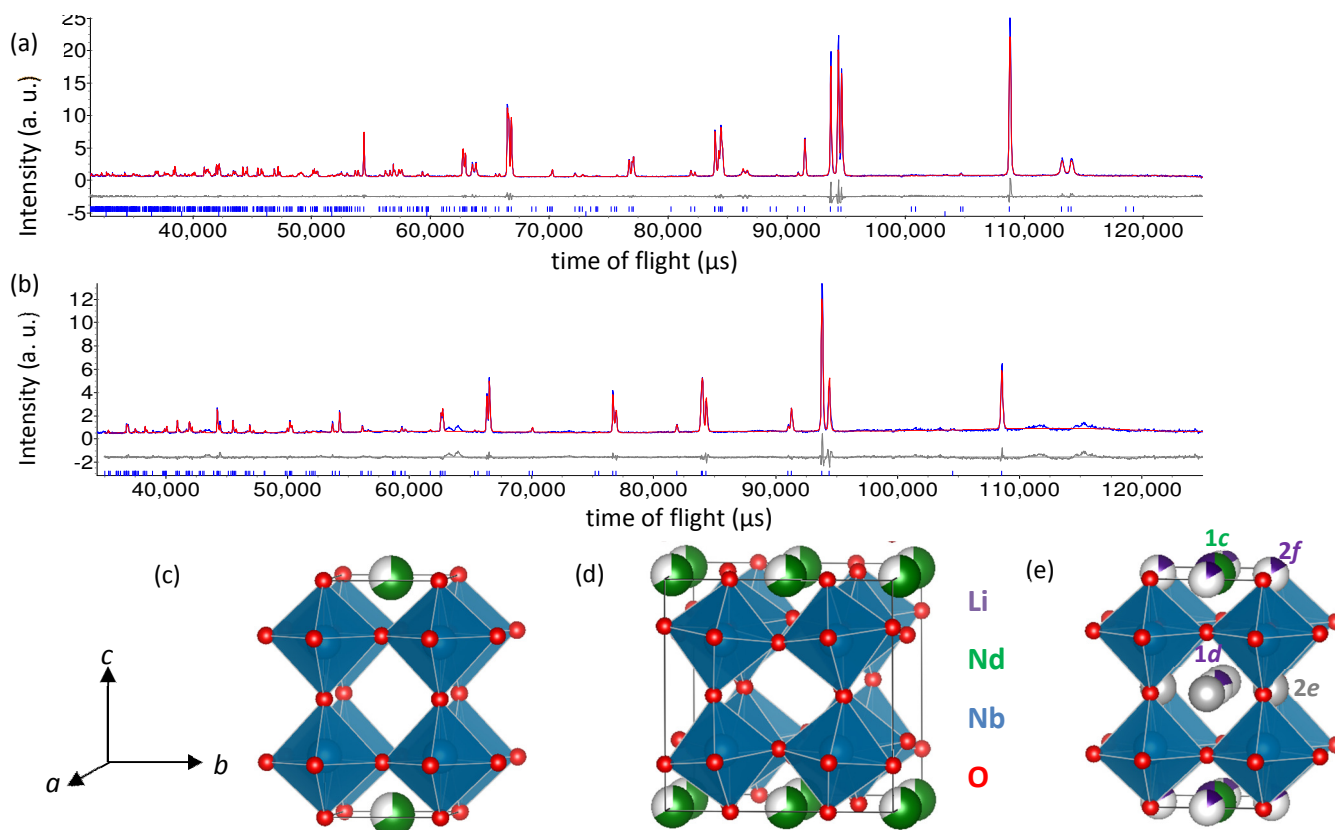
* e.e.mccabe@kent.ac.uk

Figure 1   Rietveld refinement profiles for room temperature NPD data (highest resolution 168° bank data) collected for (a) $Nd_{2/3}NbO_3$ fitted with $Cmmm$ model (with broadening of superstructure reflections) and (b) $Li_{0.26(2)}Nd_{2/3}NbO_3$, fitting with a $P4/mmm$ model, showing observed, calculated and difference profiles in blue, red and grey, respectively, with peak positions shown by blue ticks; panels (c), (d) and (e) show crystal structures of $La_{1/3}NbO_3$ (at high temperature), $Nd_{2/3}NbO_3$ and $Li_{0.31(2)}Nd_{2/3}NbO_3$ showing NbO_6 octahedra in blue and Li, Ln (Ln = La, Nd) and O sites in purple, green and red, and vacant $2e$ site in grey, respectively.

We note that electron microscopy work has been invaluable in understanding the role of microstructure resulting from variations in the oxygen sublattice and/or compositional variations in related materials,[14-15] and weak diffuse scatter has been observed in electron diffraction patterns for $Nd_{2/3}NbO_3$ consistent with variations in octahedral tilting (although it's origin couldn't be confirmed).[16] For comparison, the related non-centrosymmetric, polar model of $C2mm$ symmetry (non-standard setting of $Amm2$) was also considered. This model comprises an additional tilt ($a^-b^0c^+$) (hinted at by higher U_{11} and U_{22} values for equatorial oxide sites, ESI) and allows an in-plane polar displacement. Although this model gives a slight improvement in fit (R_{wp} decreased from 5.048% for $Cmmm$ (93 parameters) to 4.999% for $C2mm$ (105 parameters) with isotropic atomic displacement parameters), there was no visible improvement (see ESI). In the absence of any polar properties $e.g.$ second harmonic generation, it seems reasonable to assume the centrosymmetric $Cmmm$ model at 300 K, at least at the length scale probed by long-range diffraction measurements. We note that this $a^-b^0c^+$ structure was observed at a more local length scale from microscopy studies for $Ca_{0.1}La_{0.6}TiO_3$.[17]

Density functional theory (DFT) calculations on these materials are challenging due to the disordered partial occupancy of A sites in alternating layers by Nd^{3+} ions and two approaches were undertaken.† The first was to explicitly place Nd^{3+} in alternate (001) AO layers, however large supercells were required to keep the

$P4/mmm$ symmetry (see ESI). To make the computations more tractable, as a second approach we modelled the Nd 2/3 occupation in alternate layers by a divalent cation with full occupancy, to maintain charge balance, i.e. $A^{2+}_{1/2}NbO_3$. The size of this divalent A cation was varied between Be and Sr in the hope that one of these ions suitably matches the effective size of the Nd 2/3 occupation. We found that the $Ca_{1/2}NbO_3$ system simultaneously best matched i) the lattice parameters of the $P4/mmm$ explicit Nd calculations, ii) the phonons of the $P4/mmm$ explicit Nd calculations and iii) the $C2mm$ and $Cmmm$ experimental lattice parameters (see ESI). We therefore concentrate on results from this second approach, using $A^{2+}_{1/2}NbO_3$, throughout the main body of this paper. Figure 2 shows the relative energy for various structural distortions (octahedral tilts and polar displacements) as a function of cation size. These results agree well with experiment, with the largest energy gain for A = Ca (closest in radius to Nd^{3+}, ionic radii are 1.34 Å and 1.27 Å for Ca^{2+} and Nd^{3+}, respectively[18]) given by $a^-b^0c^0$, consistent with experimental work.[8] Interestingly, these calculations also predict the change in tilt axis with decreasing A cation radius, with $a^-a^-c^0$ tilts giving the greatest energy gain for the smaller Mg^{2+} analogue (consistent with the $Pbmm$ structure reported for $Tb_{1/2}TaO_3$ and $Dy_{1/2}TaO_3$). For the smallest Be^{2+} analogue, the largest energy gain results from an in-plane polar displacement, consistent with the polar $P2_1am$ structure reported for $Ho_{1/2}TaO_3$ and $Er_{1/2}TaO_3$, suggesting that the polar nature of these small Ln analogues is likely proper in origin, although interestingly, it seems
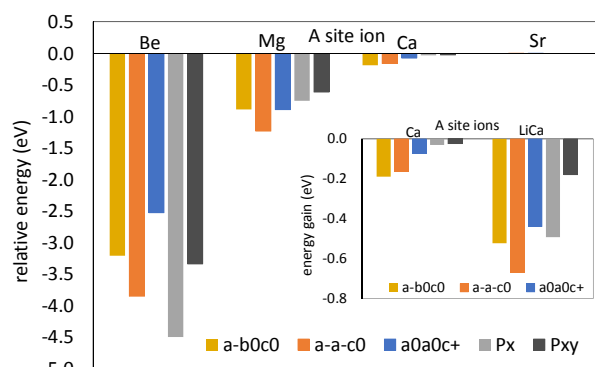
Figure 2   Energies of possible lower symmetry structures (relative to the ideal $P4/mmm$ model) for the $A^{2+}{}_{\frac{1}{2}}NbO_3$ series; inset, comparison between $Ca_{\frac{1}{2}}NbO_3$ and $Ca_{\frac{1}{2}}Li_{\frac{1}{2}}NbO_3$. Relative energies are given per 9 atom chemical formula unit.

that the polar direction (along [110] of the parent $P4/mmm$ unit cell) is dictated by the in-plane tilt axis. Allowing a combination of tilts, $a^-b^0c^+$ (to give the polar $C2mm$ model) gives a further stabilisation of 0.01 eV for $Ca_{0.5}NbO_3$. Given that such a polar structure has been observed for $Ca_{0.1}La_{0.6}TiO_3$ at shorter length scales,[17] the same may be true locally for $Nd_{\frac{1}{2}}NbO_3$. The predicted energy gain from this further symmetry lowering is very small and so not conclusive, but it is interesting to note that the driving force for the polar structure for $Ca_{0.5}NbO_3$ appears to be the combination of octahedral tilts, making it most likely improper in nature.

On reacting $Nd_{\frac{1}{2}}NbO_3$ with n-butyl lithium, a deep blue powder was formed, and XRPD suggested only a very small change in unit cell volume (see ESI). Iodometric back titrations were carried out (see ESI) to determine the stoichiometry of the lithiated phase and suggested a composition $Li_{0.34}Nd_{\frac{1}{2}}NbO_3$. Magnetic susceptibility measurements indicate that both materials remain paramagnetic to 2 K and plots of inverse susceptibility with temperature (see ESI) show reasonable agreement with Curie-Weiss behaviour for $T \geq 150$ K. The paramagnetism of $Nd_{\frac{1}{2}}NbO_3$ results from the Nd^{3+} ion ($4f^3$, $^4I_{9/2}$), and the paramagnetic moment calculated from these experimental data (2.10 μ_B per formula unit) is in excellent agreement with that expected for this $Nd_{\frac{1}{2}}$ material (2.09 μ_B per formula unit). The reductive lithiation of $Nd_{\frac{1}{2}}NbO_3$ gives some Nb^{4+} ($4d^1$, $^2D_{3/2}$) according to $Li_xNd_{\frac{1}{2}}Nb^{5+}{}_{1-x}Nb^{4+}{}_xO_3$ and the paramagnetic moment calculated for $Li_{0.34}Nd_{\frac{1}{2}}NbO_3$ is 2.67 μ_B per formula unit. This composition indicates that a third of the niobium sites are reduced to Nb^{4+} and the observed moment implies a moment of 2.88 μ_B per Nb^{4+} site. This suggests a significant orbital contribution to this Nb^{4+} moment (compare with a van Vleck moment of 3 μB for fully unquenched orbital contribution for Nb^{4+}) and is slightly larger than that that observed by Tran et al in the dimer material $Nb_2O_2F_3$ (2.24 μ_B per Nb^{4+}).[9] This preliminary magnetic analysis is consistent with the composition from iodometric titrations and further experimental work will investigate the Nb^{4+} site at a more local level.

NPD data collected for $Li_xNd_{\frac{1}{2}}NbO_3$ show a series of sharp peaks consistent with the ideal $P4/mmm$ structure ($a \approx 3.89$ Å, $c \approx 7.82$ Å) and pairs of much broader reflections consistent with distortions at the M point ($k = \frac{1}{2}\ \frac{1}{2}\ 0$). A model of $P4/mmm$ symmetry was constructed with Li^+ on the $1c$ site (partly occupying the Nd^{3+} site at $z = 0$), the $2f$ site (an interstitial site within the $z = 0$ layer), the $1d$ site (the vacant A site in the $z = 0.5$

layer) and the $2e$ site (an interstitial site in the $z = 0.5$ layer) shown in Figure 1(e), as proposed by Nadiri et al.[12] Concentrating initially on the sharp, commensurate reflections, Rietveld refinements using a single atomic displacement parameter for A sites suggested that Li^+ ions fill the remaining vacancies on the Nd^{3+} site ($1c$), with small amounts on the $2f$ interstitial site and the vacant A site ($1d$). Refining anisotropic atomic displacement parameters for the oxide sites revealed very anisotropic behaviour: both apical sites have unfeasibly high U_{11} and U_{22} values, suggesting significant displacements (either static or dynamic) within the ab plane, consistent with tilts of NbO_6 octahedra about an in-plane axis; the apical O(3) site has an unfeasibly high U_{33} value, again consistent with tilts of NbO_6 octahedra about an in-plane axis, and the high U_{11} value may also indicate some tilts about the $[001]_p$ axis (see ESI). Tilts about an in-plane axis would lower the symmetry of the system and in the absence of any peak splitting or broadening observed, it's likely that these distortions give rise to the pairs of incommensurate reflections. Mode inclusion analysis[19] (considering only the sharp commensurate reflections) suggested that the fit improved for models that allowed out-of-plane displacements or tilts about $[001]_p$ but allowing such distortions predicted intensity where none is observed experimentally. Allowing the apical oxide sites to disorder within the ab plane (moving them from $1a$ and $1b$ sites to $4i$ and $4j$ sites) improved the fit and gave more feasible atomic displacement parameters (although still high, likely reflecting deficiencies with the model due to incommensurate modulations in the structure). Final refinement profiles and details are given in Figure 1 and and Table 1 (and ESI). This refinement suggests a stoichiometry of $Li_{0.26(2)}Nd_{\frac{1}{2}}NbO_3$ (in reasonable agreement with iodometric titrations) and a slightly reduced out-of-centre displacement of Nb cations (consistent with partial reduction to $4d^1$ Nb^{4+} ions) and further characterisation work is underway to confirm this.

Table 1   Refinement details from Rietveld refinements using room temperature NPD data collected for $Li_{0.26(2)}Nd_{\frac{1}{2}}NbO_3$ with disordered $P4/mmm$ model with $a = 3.8857(1)$ Å, $c = 7.8200(2)$ Å, volume = 118.070(8) Å^3; R_{wp} = 10.60%, R_p = 8.01%, χ^2 = 18.94.

Atom	site	x	y	z	occupancy	$U_{iso} \times 100$ (Å^2)
Nd/Li(1)	1c	0.5	0.5	0	0.667/0.33(4)	0.5(1)
Li(2)	2f	0.5	0	0	0.04(2)	0.5(1)
Li(3)	1d	0.5	0.5	0.5	0.17(2)	0.5(1)
Nb	2g	0	0	0.2611(3)	1	-
O(1)	4j	0.060(9)	0.060(9)	0	1	-
O(2)	4k	0.078(1)	0.078(1)	0.5	1	-
O(3)	4i	0	0.5	0.2294(7)	1	-

	$U_{ij} \times 100$ (Å^2)				
Atom	U_{11}	U_{22}	U_{33}	U_{12}	U_{13}	U_{23}
Nb	0.5(3)	1.6(2)	1.0(2)	-1(1)	-0.3(2)	2.0(7)
O(1)	6(1)	5(2)	0.0(5)	-0.5(9)	1(8)	0(8)
O(2)	0.02(7)	4(1)	4.0(7)	-0.4(4)	2.6(7)	5(1)
O(3)	7.3(4)	0.1(1)	13.8(4)	0.0(2)	0.2(5)	0.0(1)

Attempts to index the pairs of broad reflections with commensurate supercells weren't successful and they couldn't be fitted by likely impurity phases. These peaks are close to the peak positions expected for M-point distortions (i.e. $a^-a^-c^0$ octahedral tilts) and could be reasonably well fitted by LeBail

refinements using an incommensurate k vector k = (0.4544 0.4544 0) (see ESI). The absence of similar broad peaks in XRPD data (see ESI) suggests that they arise from either the distribution of light Li^+ ions, and/or the oxide sublattice. Similar diffuse incommensurate scattering has been investigated in related materials, particularly by electron microscopy, and ascribed to octahedral tilt twinning or modulations in composition.[10-11, 20-22] The broad nature of these reflections in our NPD data makes it difficult to differentiate between possible models and we can't confirm the crystal structure. The best fits were obtained with ($a^-a^-c^0$)-like tilts but full analysis is on-going and will be complemented by microscopy and local probes such as ssNMR. It's clear that Li^+ insertion alters the tilt pattern and it's likely this is primarily due to tolerance factor arguments, with Li^+ content and distribution tuning the nature and length scale of the octahedral tilts; future work will investigate the influence of lithiation conditions on structure and properties.

First principles calculations† were similarly performed on an effective $Li_{1/2}Ca_{1/3}NbO_3$ system, with Li^+ completely occupying the $1d$ sites as inferred by the Rietveld refinements. Calculations were performed in absence of spin or charge ordering, and it was found that the gain in energy for all of modes substantially increased as compared to $Nd_{1/3}NbO_3$. Interestingly, the most favourable direction for the in-plane tilts becomes the $[110]_p$ (i.e. $a^-a^-c^0$), with $a^0a^0c^+$ tilts and an in-plane polarisation also giving sizeable stabilisations (Figure 2). The ground state was found to be polar $P2_1am$ ($a^-a^-c^+$). This mirrors the results of calculations above for $A_{1/2}NbO_3$ showing the effect of decreasing A^{2+} cation radius and suggests that reductive lithiation reactions, which increase the average B radius, can tune the structural chemistry and polar nature of these systems by steric (tolerance factor) effects.

This work has highlighted the structural chemistry of A-site deficient perovskite materials $Ln_{1/3}NbO_3$ with computational work illustrating the possibility of tuning between proper and hybrid-improper like behaviour by choice of Ln^{3+} and also by reductive cation-insertion reactions. Our calculations suggest that this results from steric effects explained by the perovskite tolerance factor. Reductive lithiation reactions can give variable lithium contents and further experimental work (synthetic, as well as characterisation using more local probes such as ssNMR) will focus on exploring this and understanding how the Li^+ distribution influences the oxide sublattice and structure. Whilst polar structures are observed for these systems, the possibility of reversing polarisation has yet to be demonstrated experimentally or investigated theoretically.

Conflicts of interest

There are no conflicts to declare.

References

1. Bousquet, E.; Dawber, M.; Stucki, N.; Lichtensteiger, C.; Hermet, P.; Gariglio, S.; Triscone, J.-M.; Ghosez, P., *Nature* **2008,** *452*, 732-736.
2. Benedek, N. A.; Rondinelli, J. M.; Djani, H.; Ghosez, P.; Lightfoot, P., *Dalton Trans.* **2015,** *44*, 10543-10558.
3. Campbell, B. J.; Stokes, H. T.; Tanner, D. E.; Hatch, D. M., *J. Appl. Cryst.* **2006,** *39*, 607-614.
4. Kennedy, B. J.; Howard, C. J.; Kubota, Y.; Kato, K., *J. Solid State Chem.* **2004,** *177*, 4552 - 4556.
5. Azough, F.; Freer, R., *J. Am. Ceram. Soc.* **2010,** *9* (5), 1237-1240.
6. Knapp, M. C.; Woodward, P., *J. Solid State Chem.* **2006,** *179*, 1076-1085.
7. Zhou, Q.; Saines, P. J.; Sharma, N.; Ting, J.; Kennedy, B. J.; Zhang, Z.; Withers, R. L.; Wallwork, K. S., *Chem. Mater.* **2008,** *20*, 6666-6676.
8. Zhang, Z.; Howard, C. J.; Kennedy, B. J.; Knight, K. S.; Zhou, Q., *J. Solid State Chem.* **2007,** *180*, 1846-1851.
9. Tran, T. T.; Gooch, M.; Lorenz, B.; Litvinchuk, A. P.; Sorolla, M. G.; Brgoch, J.; Chu, P. C. W.; Guloy, A. M., *J. Am. Chem. Soc.* **2015,** *137*, 636-639.
10. King, G.; Garcia-Martin, S.; Woodward, P. M., *Acta Crystallogr. Sect. B-Struct. Sci.* **2009,** *65*, 676-683.
11. Guiton, B. S.; Davies, P. K., *Nat. Mater.* **2007,** *6* (8), 586-591.
12. Nadiri, A.; Flem, G. l.; Delmas, C., *J. Solid State Chem.* **1988,** *73*, 338-347.
13. Roudeau, S.; Weill, F.; Pechev, S.; Bassat, J.-M.; Grenier, J.-C., *C. R. Chimie* **2008,** *11*, 734-740.
14. Kresse, G.; Hafner, J., *Phys. Rev. B* **1993,** *47*, 558.
15. Kresse, G.; Furthmuller, J., *Comput. Mater. Sci.* **1996,** *6*, 15.
16. Perdew, J. P.; Ruzsinszky, A.; Csonka, G. I.; Vydrov, O. A.; Scuseria, G. E.; Constantin, L. A.; Zhou, X.; Burke, K., *Phys. Rev. Lett.* **2008,** *100*, 136406.
17. Danaie, M.; Kepaptsoglou, D.; Ramasse, Q.; Ophus, C.; Whittle, K. R.; Lawson, S. M.; Pedrazzini, S.; Young, N. P.; Bagot, P. A. J.; Edmondson, P. D., *Inorg. Chem.* **2016,** *55*, 9937-9948.
18. Shannon, R. D., *Acta Cryst.* **1976,** *A32*, 751.
19. McCabe, E. E.; Free, D. G.; Mendis, B. G.; Higgins, J. S.; Evans, J. S. O., *Chem. Mater.* **2010,** *22*, 6171-6182.
20. Azough, F.; Kepaptsoglou, D.; Ramasse, Q. M.; Schaffer, B.; Freer, R., *Chem. Mat.* **2015,** *27* (2), 497-507.
21. Abakumov, A. M.; Erni, R.; Tsirlin, A. A.; Rossell, M. D.; Batuk, D.; Nenert, G.; Van Tendeloo, G., *Chem. Mat.* **2013,** *25* (13), 2670-2683.
22. Garcia-Martin, S.; Alario-Franco, M. A.; Ehrenberg, H.; Rodriguez-Carvajal, J.; Amador, U., *Journal of the American Chemical Society* **2004,** *126* (11), 3587-3596.